

Environmental Flows Term Project

GROUP 1



AW WEI NA, CHERIE (A0040143B)

NG WEN HAO (A0169308X)

LI ZHI (A0169388H)

WONG PUI YEE (A0056182H)

ZHANG YANAN (A0083854W)

Contents

1.	Objective.....	1
2.	Background	1
3.	Model set-up	1
3.1	Thin dams and dry points	1
3.2	Observation points	2
4.	Model Calibration and Validation	3
4.1	Parameter Selection	3
4.1.1	Time step and simulation period	3
4.1.2	Manning's roughness coefficient	4
4.1.3	Thatcher-Harleman time lag	5
4.1.4	Horizontal diffusivity	5
4.1.5	Heat flux model	6
4.1.6	Wind input	6
4.1.7	Discharge	6
4.1.8	Initial and boundary conditions	7
4.2	Model Validation	7
4.2.1	Water level	7
4.2.2	Current velocities	7
5.	Impact Assessment	8
5.1	Scenarios	9
5.2	Results	9
5.3	Impacts	10
6.	Conclusion and Recommendations	10
7.	References	11

1. Objective

The objective of this report is to provide a preliminary evaluation with the use of Delft3D on which of the two locations, location 1 or 2 (Figure 1-1), is the most advantageous to accommodate a new plant, which will be discharging water with discharge values equivalent to discharge C and M. This preliminary assessment will be carried out in terms of the impact to the thermal regime in the vicinity of Jurong Island.



Figure 1-1: Illustration of location 1 and 2 with respect to Jurong Island

2. Background

Jurong Island is an offshore island in the southwest of Singapore and it holds many global petroleum, petrochemical and specialty chemical plants. These plants mostly have water intakes, mainly used for fire-fighting or cooling purposes, and also thermal discharges as a result of the cooling processes.

3. Model set-up

3.1 THIN DAMS AND DRY POINTS

For this project, thin dams and dry points were edited in the areas (A, B, C and D) circled in red (Figure 3-1). With reference to the updated land boundary, dry points and thin dams were added and removed accordingly. A dry point was added if the area occupied is about $\geq 50\%$ of the grid cell. The final model grid for the corresponding areas are shown in Figure 3-2.

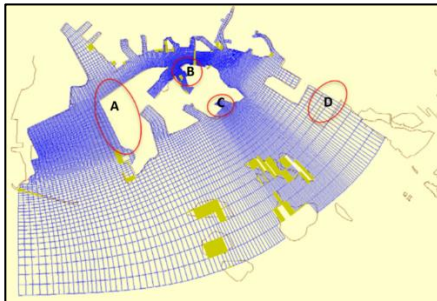


Figure 3-1: Existing thin dams and dry points model grid

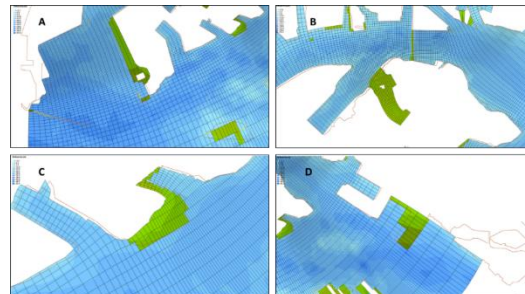


Figure 3-2: Thin dams and dry points for areas in circled in red

3.2 OBSERVATION POINTS

Figure 3-3 shows the overview of the observations points included in the model domain. In order to assess the temperature changes at location 1 and 2, additional points were added in the close vicinity of both locations as well as at a distance of approximately 500 meters away these locations to verify the temperature spin up at this area of interest. In addition, observations points at 5 locations (Ferry Terminal, Banyan Buoy, Sawa Buoy, West Jurong and Obs10) were included for model validation purposes. Several additional observation points were included in the vicinity of Ferry Terminal and West Jurong for additional assessment (refer to Section 4.2.2). The additional observations points are illustrated in Figure 3-4.

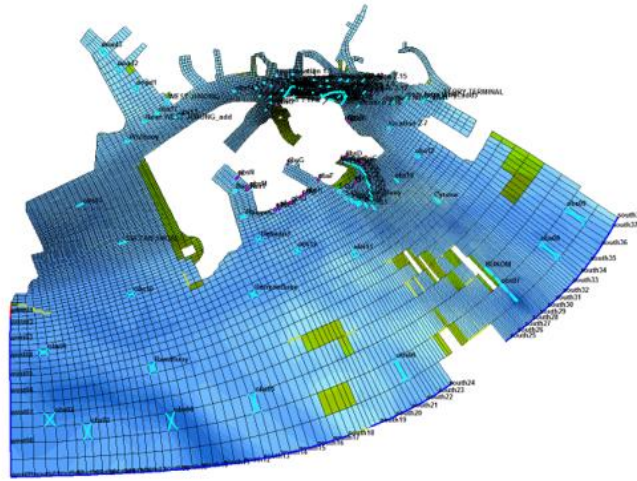


Figure 3-3: Overview of observation points in model domain

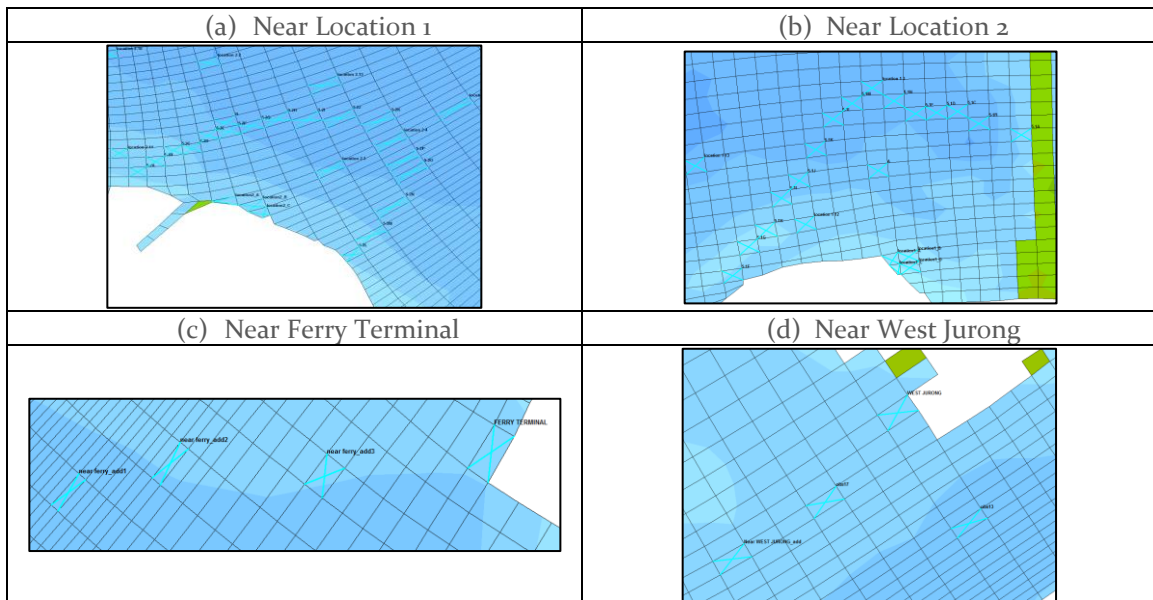


Figure 3-4: Additional observation points in the vicinity of (a) Location 1, (b) Location 2, (c) Ferry Terminal, and (d) West Jurong

4. Model Calibration and Validation

4.1 PARAMETER SELECTION

4.1.1 TIME STEP AND SIMULATION PERIOD

A time step of one minute was selected for the model simulation after considering the trade-off between computational time and model stability. The simulation period for the assessment was chosen to be 2 August 2017 0000h to 1 September 2017 0000h, which is considered as neap-to neap over a month in Singapore (illustrated in Figure 4-1). The simulation period also was selected after assessing the model spin up time for several parameters.

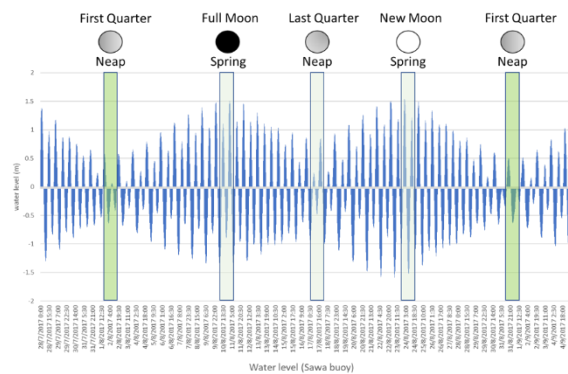


Figure 4-1: Illustration of a neap-to-neap simulation period

Stability and spin up time

Model spin up time was checked through visual inspection of the water level, x-component of depth averaged velocity and temperature at Ferry Terminal, Banyan Buoy, Sawa Buoy, West Jurong, Location 1a, Location 1b and Obs10 (Figure 4-2, Figure 4-3, Figure 4-4). For water level and velocity, large variations were noted in the beginning of the simulation, and the readings stabilized after approximately 3 days. In the peaks and troughs, some small disturbances persist until the end of the simulation. This implies that transient solutions in the Delft3D computations does not dissipate during the simulation which is possibly due to the limitations in grid quality. For temperature, the model seems to be stable after approximately 5 weeks.

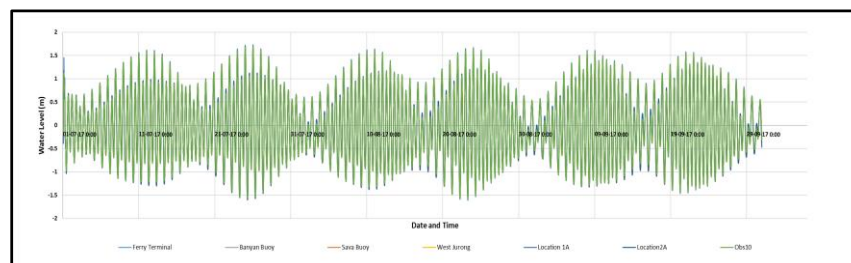


Figure 4-2: Water level at various locations

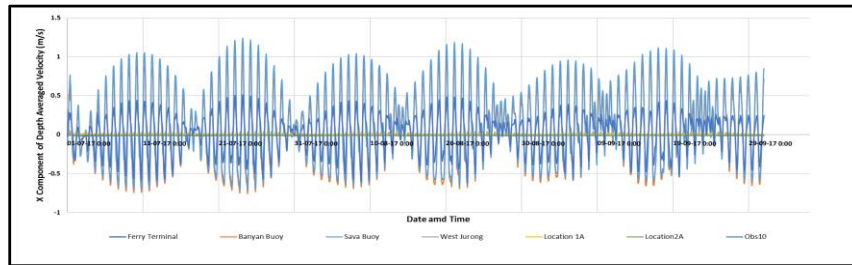


Figure 4-3: x-component of depth averaged velocity at various locations

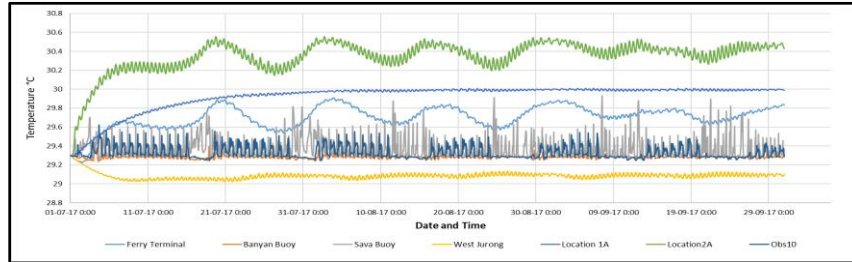


Figure 4-4: Temperature at various locations

Additional checks for model spin up in terms of temperature were also performed at the additional observation points at 2 areas of interest (Location 1 and 2) for the impact assessment. Similar to the analysis above, the spin up time is approximately 5 weeks at these points (Figure 4-5).

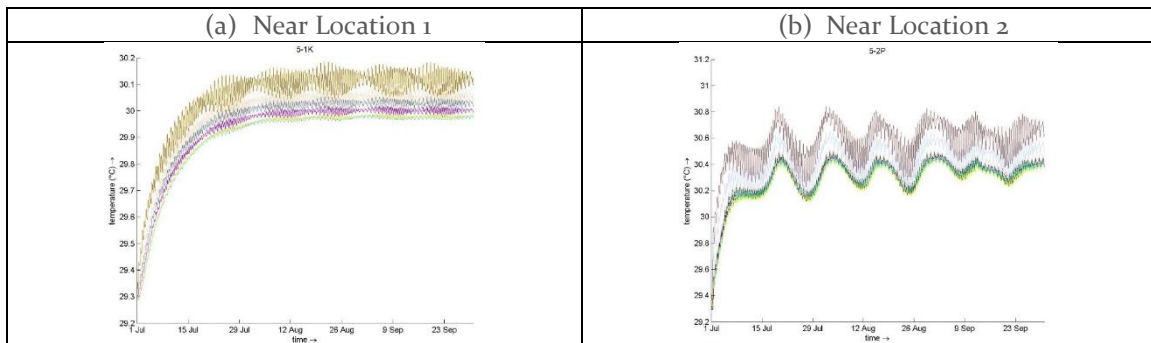


Figure 4-5: Temperature at additional observation points around (a) location 1, and (b) location 2

4.1.2 MANNING'S ROUGHNESS COEFFICIENT

In the selection of the Manning's coefficient, a sensitivity analysis was carried out with the values 0.02, 0.03 and 0.04. The Manning roughness coefficient is selected to be 0.03. The sensitivity analysis was carried out by comparing the water level and depth averaged velocity components with the actual data provided. For water levels, 0.02 and 0.03 have higher correlations than 0.04. The ranking from the water levels is only indicative but may not be a critical factor given that the values for the correlation for all three Manning's are considered very high.

When comparing the velocity components, 0.03 and 0.04 have better correlations than 0.02. This shows that 0.02 is less accurate in representing the velocities and will not be considered as our choice. It is also considered that the Manning's coefficient to choose should still represent the physical conditions of the ocean floor. Studies show that Manning's coefficient does not go beyond 0.03 for

oceanic flows (Talea Mayo, 2014). Coefficients above that number typically applies to vegetation and crops (S. Bunya, 2010). Hence, the coefficient of 0.03 was used.

Table 4-1: Summary of correlation and root mean square error (RMSE) values for validation points for Manning's coefficient of 0.02, 0.03 and 0.04

Water Level						Vel-x component					
Manning coefficient		0.02		0.03		0.02		0.03		0.04	
Location	Correlation	Root Mean Square Error (RMSE)	Correlation	Root Mean Square Error (RMSE)	Correlation	Location	Correlation	Root Mean Square Error (RMSE)	Correlation	Root Mean Square Error (RMSE)	Correlation
banyan	0.99968	0.01902	0.99964	0.02124	0.99736	banyan	0.994888207	0.086126166	0.998440322	0.066828429	0.9986962
ferry	0.99945	0.02436	0.99957	0.02153	0.99956	ferry	0.639139809	0.004403648	0.788830997	0.003715712	0.8602701
obs10	0.99968	0.01896	0.99916	0.03227	0.99476	obs10	-0.269140215	0.156888755	-0.337686207	0.156226769	-0.389125
sawa	0.99978	0.01517	0.99987	0.01207	0.99978	sawa	0.992013079	0.061560931	0.99570431	0.057311599	0.9966137
westjurong	0.99937	0.02716	0.99896	0.03623	0.99462	westjurong	0.750106646	0.013672522	0.835359208	0.011645435	0.8828772
Average	0.99959	0.02093	0.99944	0.02467	0.99721	Average	0.621401506	0.064530408	0.656129726	0.059145589	0.6698665

Vel-y component					
Manning coefficient		0.02		0.03	
Location	Correlation	Root Mean Square Error (RMSE)	Correlation	Root Mean Square Error (RMSE)	Correlation
banyan	0.993719215	0.036342476	0.996753311	0.02886904	0.996256
ferry	0.487646931	0.00668101	0.683309703	0.004895173	0.794237
obs10	-0.239642773	0.109690387	-0.181435855	0.087789107	0.059123
sawa	0.984891327	0.062728441	0.989054387	0.06623214	0.99073
westjurong	0.618378905	0.020094822	0.763362192	0.020030636	0.835519
Average	0.568987231	0.047107427	0.650208748	0.041563219	0.735173

4.1.3 THATCHER-HARLEMAN TIME LAG

In this project, a Thatcher-Harleman time lag of 360 minutes, i.e. 6 hours, was applied, which is the approximate period of half a tidal cycle observed from the model. This is likely to be a redundant feature in the model, as the effect of this input is only noticeable near the boundary which is away from the area of interest near the new discharge locations.

4.1.4 HORIZONTAL DIFFUSIVITY

Horizontal eddy diffusivity largely relies on the flow and grid size used in simulation. In area of interest, the grid size in general are tens of meters or even less, which result in a typical diffusivity range of 1-10m²/s (Deltares, 2013). Hence, horizontal diffusivity of 1 m²/s, 5 m²/s and 10 m²/s were tested. As shown in Figure 4-6, temperature profile at Location 1 with aforementioned horizontal diffusivity values were plotted. It was noted that horizontal diffusivity of 1 m²/s gives high fluctuations and therefore, horizontal diffusivity of 1 m²/s was eliminated from the selection. Two sensitivity tests were simulated with horizontal diffusivity 5 m²/s and 10 m²/s (Figure 4-7 and Figure 4-8). The model results showed that higher temperature was obtained with horizontal diffusivity of 5 m²/s than 10 m²/s for both tested locations. Therefore, horizontal diffusivity of 5 m²/s was chosen for impact assessment scenario as it was a relatively worse case.

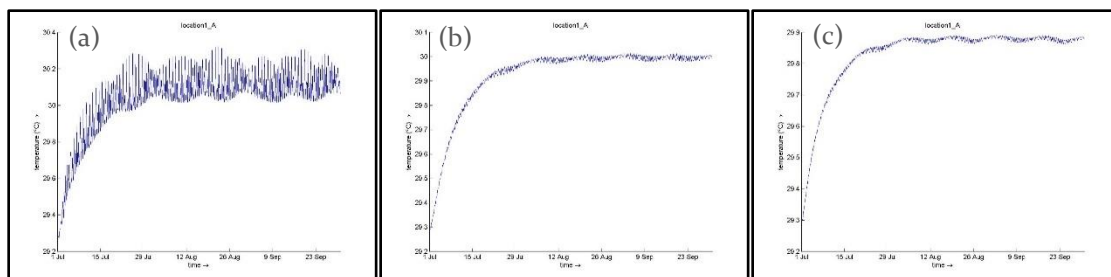


Figure 4-6: Temperature profile at Location 1 with different horizontal diffusivity (a) 1 m²/s (b) 5 m²/s (c) 10 m²/s

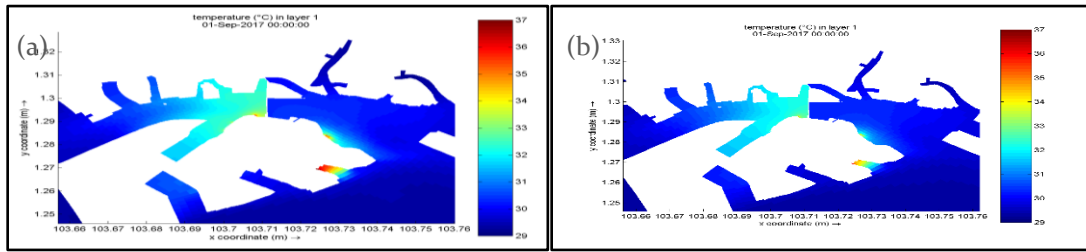


Figure 4-7: Sensitivity test 1 with horizontal diffusivity of (a) 5 m/s² and (b) 10 m/s²

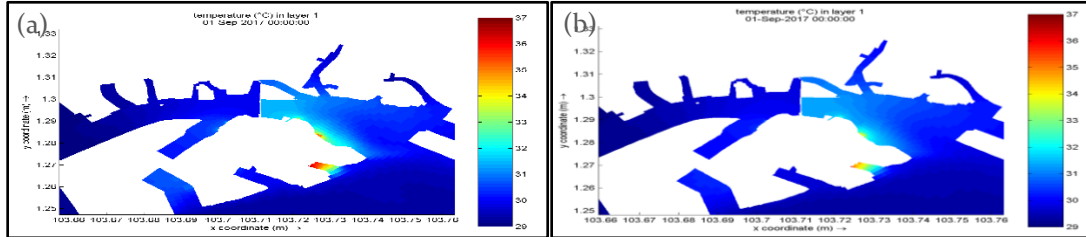


Figure 4-8: Sensitivity test 2 with horizontal diffusivity of (a) 5 m/s² and (b) 10 m/s²

4.1.5 HEAT FLUX MODEL

In the case of modelling the effect of a thermal discharge, it is sufficient to compute the excess temperature and decay. Hence, the heat flux model chosen in this analysis was the excess temperature model that computes the heat exchange flux at the air-water interface. The background temperature applied was 28.5°C (National Environmental Agency, 2017).

4.1.6 WIND INPUT

The simulation period lies in the Southwest Monsoon (July to September), where wind directions are mainly from southerly to southeasterly. Hence, the chosen wind input is wind of approximately 10.89 km/h or 3.025 m/s, blowing from the South direction (National Environmental Agency, 2017).

4.1.7 DISCHARGE

18 discharge points (A to Q) were provided and included in the model simulation. The quantities, temperature and locations of the discharges are presented in Figure 4-9. The water depth at these 18 discharges were also checked and these locations were verified to be in the fully flooded location. Hence, the “normal” discharge function was used.

Discharge Point	Quantity (m ³ /h)	Temperature °C
A	130,000	38.0
B	100,000	38.0
C	54,000	39.0
D	100,000	38.0
E	141,000	36.0
F	15,000	31.5
G	14,100	34.5
H	18,000	37.0
I	4,500	38.0
J	41,000	35.0
K	30,000	38.0
L	12,000	39.0
M	39,000	39.0
N	21,000	36.5
O	21,000	39.0
P	24,000	39.0
Q	9,000	37.0

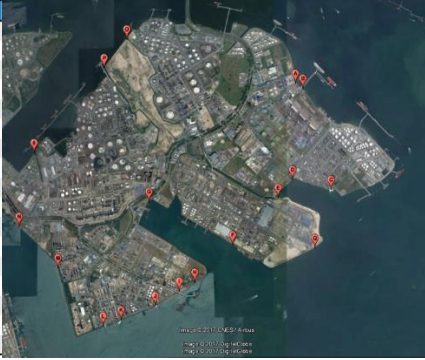


Figure 4-9: Quantity, temperature and locations of discharges A to Q

4.1.8 INITIAL AND BOUNDARY CONDITIONS

The initial water levels were set to 0 and allowed to spin up on its own. The initial temperature is set to the average water temperature at 29.3°C (World sea temperature, 2017) to reduce the spin-up time

The water current and level boundary conditions were used as provided in the time series, whilst the transport condition temperatures were set at 29.3°C.

4.2 MODEL VALIDATION

As part of the parameter selection for Manning's roughness coefficient (refer to Section 4.1.2), validation of the model for water level and current velocities were carried out against actual field data at 5 locations.

4.2.1 WATER LEVEL

The validation results for water level show that the correlation factor ranges from 0.99896 to 0.99987, which is close to 1 (refer to Table 4-1). This shows that there is good correlation between the water level simulated in the model and the actual water level measurements all at 5 locations.

4.2.2 CURRENT VELOCITIES

The validation results for current velocities show that correlation factor ranges from -0.33769 to 0.99844 for the x component and -0.18143 to 0.99675 for the y-component (refer to Table 4-1). The RMSE values for the 5 locations all fall between ± 0.2 m/s, hence the validation results in terms of RMSE are acceptable. From the results, it can be seen that the correlation results for Banyan Buoy and Sawa Buoy are close to 1, showing good correlation. However, lower correlations are seen for the remaining 3 locations. The correlation factor for West Jurong is approximately 0.76 to 0.84, can be considered acceptable, fulfilling the criteria of 0.75 to 0.85. However, Ferry Terminal has correlation factors which are only borderline acceptable and there is poor correlation at Obs10.

After further assessment, it can be assessed that West Jurong and Ferry Terminal have lower correlation due to the fact that the location is situated at the grid cell next to the coast lines where a coarser grid size was used. Within the grid, there may be steep bathymetry changes and this results in an averaged reading that is not reflective of the true result at the exact location. This problem can be resolved by either reducing the grid size or choosing an observation point that is away from the coastal point. It can be seen that the correlation increases when adopting another observation point, near ferry (refer to Figure 3-4 and Table 4-2).

Table 4-2: Comparison of correlation and root mean square error (RMSE) values at Ferry Terminal and near ferry for Manning's coefficient of 0.02, 0.03 and 0.04

Water Level			Velocity (x-comp)			Velocity (y-comp)		
Manning coefficient	0.03		Manning coefficient	0.03		Manning coefficient	0.03	
Location	Correlation	Root Mean Square Error (RMSE)	Location	Correlation	Root Mean Square Error (RMSE)	Location	Correlation	Root Mean Square Error (RMSE)
banyan	0.99964	0.02124	banyan	0.998440322	0.066828429	banyan	0.996753311	0.02886904
ferry	0.99957	0.02153	ferry	0.788830997	0.003715712	ferry	0.683309703	0.004895173
near_ferry	0.99991	0.01303	near_ferry	0.95507	0.023455	near_ferry	0.86635	0.013
obs10	0.99916	0.03227	obs10	-0.337686207	0.156226769	obs10	-0.181435855	0.087789107
sawa	0.99987	0.01207	sawa	0.99570431	0.057311599	sawa	0.989054387	0.06623214
westjurong	0.99896	0.03623	westjurong	0.835359208	0.011645435	westjurong	0.763362192	0.020030636

Subsequently, the reason for the uncharacteristic correlation in obs10 is due to the presence of an eddy in the region. It can be seen by plotting the velocities, where it shows a visible eddy spanning the region between Tuas finger and the west of Jurong Island land mass (Figure 4-10). The occurrence of the eddy is due to the model trying to conserve the mass that is going in and out of the L-shaped channel around the west to north part of Jurong Island. Therefore, observation points around obs10 will not be able to achieve a steady state comparison between numerical and true data and will mostly reflect a random result.

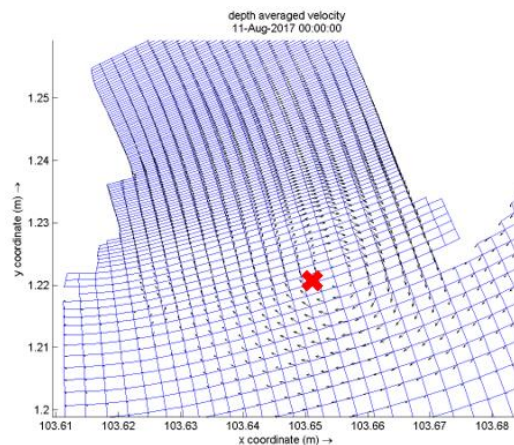


Figure 4-10: Snapshot of eddy formation in the vicinity of obs10

5. Impact Assessment

This preliminary impact assessment serves as an initial check for typical industry analysis, and is termed as a scoping exercise. Two locations, location 1 or 2, will be evaluated separately to determine which location is the most advantageous to accommodate a new plant with a thermal discharge. This preliminary assessment will be carried out in terms of the impact to the thermal regime in the vicinity of Jurong Island.

The new discharge will be discharging water with discharge values equivalent to discharge C and M with the following values:

- Discharge $Q = 93,000 \text{ m}^3/\text{h}$ or $25.8 \text{ m}^3/\text{s}$
- Temperature = 39°C



Figure 5-1: Locations 1 and 2 with respect to Jurong Island

5.1 SCENARIOS

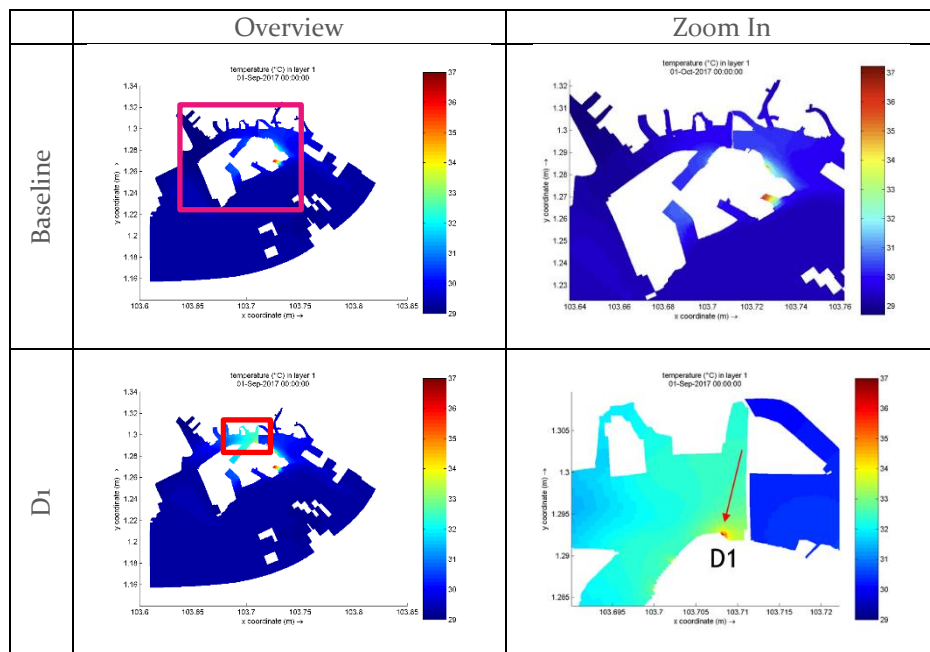
For the impact assessment, 3 scenarios have been simulated and details of the scenarios are tabulated in Table 5-1.

Table 5-1: Summary of scenarios simulated for impact assessment

Scenario	Description
Baseline	<ul style="list-style-type: none"> Includes Discharges A to Q
D ₁	<ul style="list-style-type: none"> Includes Discharges A to Q Includes new discharge at location 1
D ₂	<ul style="list-style-type: none"> Includes Discharges A to Q Includes new discharge at location 2

5.2 RESULTS

The results for the 3 scenarios simulated are presented in Figure 5-2. It can be seen that with the introduction of the new thermal discharge at either location 1 or 2, there would be an increase in the temperature of the ambient marine water in the vicinity of the discharge. The difference in temperature from the baseline scenario is also presented in Figure 5-3. It can be assessed that it will result in a larger temperature change from the baseline condition if the new thermal discharge is located at location 1, as compared to that at location 2.



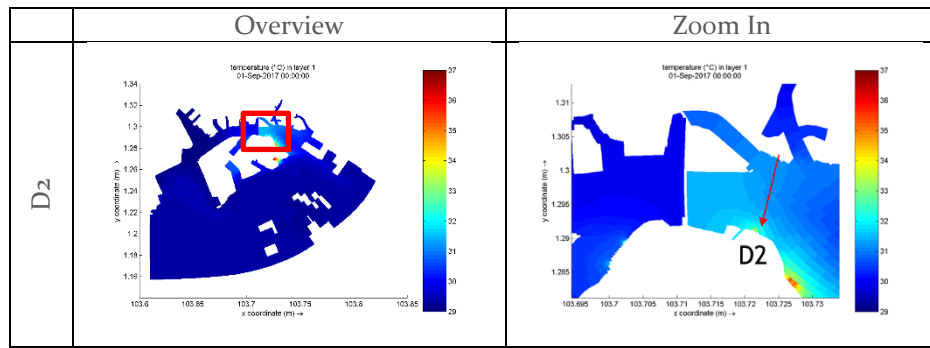


Figure 5-2: Model results (temperature) at last timestep (1 Sep 2017 0000h) for 3 scenarios

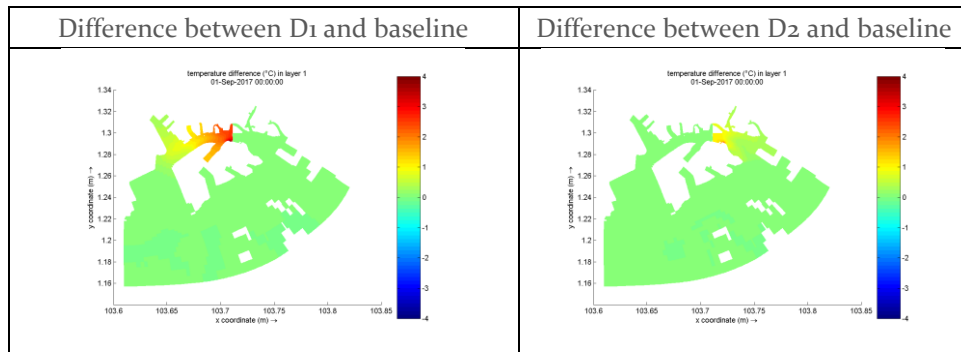


Figure 5-3: Model results (temperature difference) at last timestep (1 Sep 2017 0000h) for 3 scenarios

5.3 IMPACTS

The increase in marine water temperature as a result of the new thermal discharge may lead to some negative impacts on certain socio-economic receptors in the vicinity. Firstly, as there are several shipyards such as Jurong Shipyard and STM in the vicinity of Location 1, the new thermal at Location 1 may lead to shipyard vessel corrosion as this is an endothermic process.

Additionally, it can be assumed that there would be water intakes such as cooling water intakes for the 18 plants that we have simulated the thermal discharges. Hence, an increase in water temperature would affect the cooling processes, since the water would be taken in might not be suitable for cooling or the intake water would have to be cooled further.

6. Conclusion and Recommendations

Based on the above considerations on the extent of the temperature change from the model results and the potential impacts which may arise from the change in temperature, it can be concluded that locating the new thermal discharge at location 2 has lesser impact on the thermal regime and would be a better choice as compared to location 1.

However, there may be some limitations relating to model simulated in this assessment. Some of the limitations are as follows:

1. A depth averaged model is simulated in this assessment. However, as there may be stratification issues relating to temperature changes, a 3D model could be used instead to obtain more accurate model results.
2. Assumptions on boundary and initial conditions for temperature and wind parameters may not be fully representative of the real-life conditions
 - a. Uniform values were applied across the time domain for boundary conditions and space domain for initial conditions for temperature in this assessment. Uniform values for wind were applied as well. More accurate model results could be obtained if actual conditions were applied instead.
3. The assessment only included the 18 discharges which were provided and did not include other discharges in the grid domain. In addition, uniform discharge values assumed and this may not be fully representative of the real-life conditions.

Therefore, it is recommended that the above discussion points should be taken into consideration during the full impact assessment phase.

7. References

Deltares. (2013). *Delft3D-FLOW Manual*. Delft:Deltares.

National Environmental Agency. (2017). Retrieved from <http://www.nea.gov.sg/>

S. Bunya, J. D. (2010). A high-resolution coupled riverine flow, tide, wind, wind wave, and storm surge model for southern Louisiana and Mississippi. Part I: model development and validation. *Monsoon Weather Review*, 345-377.

Talea Mayo, T. B. (2014). Data assimilation within the Advanced Circulation (ADCIRC) modeling framework for the estimation of Manning's friction coefficient. *Ocean Modelling*, 43-58.

World sea temperature. (2017). Retrieved from <https://www.seatemperature.org/asia/singapore/singapore-july.htm>